JOURNAL OF GUIDANCE, CONTROL, AND DYNAMICS
Vol. 28, No. 6, November–December 2005

Effect of Electrodynamic Forces on the Orbital Dynamics of Tethered Satellites

Eric L. M. Lanoix*
Titan Corporation, Houston, Texas 77058
Arun K. Misra†
McGill University, Montreal, Quebec H3A 2K6, Canada
Vinod J. Modi‡
University of British Columbia, Vancouver, British Columbia V6T 1Z4, Canada
and
George Tyc§
Macdonald Dettweiler Associates, Richmond, British Columbia V6V 2J3, Canada

Tethered satellites have a vast potential for space applications. If the tether is conductive, electrodynamic forces result from the motion of the conductive tether relative to the magnetic field of the Earth. The long-term effect of electrodynamic forces on the equinoctial orbital elements of a tethered system is studied with use of a detailed model of the Earth's magnetic field as well as of the tether dynamics. A detailed gravity and aerodynamic model is used. In all cases studied, bare tethers induce larger electrodynamic forces than insulated tether systems. The results show that Lorentz forces can remove a satellite from orbit more effectively than air drag if a conductive tether is attached to it. A simple control law is used to stabilize tether librations caused by electrodynamic forces. Such an approach for junk removal is practical if the satellite mass is greater than 100 kg or so.

Introduction

THE first in-flight experiments on space tethers took place in 1966.[1] During the last months of the Gemini program, two different crews used a 30-m Draco tether to demonstrate the spin and gravity gradient stabilization of tethers. Following a 15-year hiatus, the 1980s and 1990s saw the rebirth of tethered flight.[2,3] Missions such as Charge 2A and 2B, Observations of Electric-Field Distribution in the Ionospheric Plasma—a Unique Strategy (Oedipus-A), Oedipus-C, Tethered Satellite System (TSS-1), TSS-1R (reflight of TSS-1), Small Expandable Deployer System (SEDS-1), SEDS-2, Plasma Motor Generator (PMG), and Tether Physics and Survivability (TiPS) have provided extensive experimental verification for the theoretical models developed over the 1970s and 1980s.

Among other things, these missions have demonstrated generation of electric current (TSS-1R), tethered momentum transfer (SEDS-1), deployment control (SEDS-2), long-term survivability (TiPS), and electrodynamic orbital boost (PMG). Numerous potential applications of space tethers have been proposed. The interested reader is referred to Ref. 2 for a comprehensive survey on the topic.

Several studies on the dynamics and control of space tethered systems have been conducted. Many of them have considered detailed models of environmental forces.[4] However, most tethered missions flown to date have been carried out over short periods of time: less than a week. Hence, there was no motivation to study the long-term orbital and attitude dynamics of such systems. However, the flight of TiPS (launched in 1996) has paved the way for much longer missions.[5]

Received 22 July 2003; revision received 1 October 2004; accepted for publication 28 October 2004.

*Senior Engineer, Astronautics Engineering Unit.
†Professor and Chair, Department of Mechanical Engineering. Associate Fellow AIAA.
‡Professor Emeritus, Department of Mechanical Engineering. Fellow AIAA.
§Manager, Small Satellites.

Studying the long-term dynamics of TiPS has motivated the development of new models with enough detail to simulate the flight of tethered spacecraft accurately over long periods of time. One such model developed by the authors is discussed in detail in Refs. 6 and 7 and will be outlined in the theory section. This formulation has proved quite accurate in predicting the long-term evolution of the orbital trajectory and of the librations of tethered spacecraft.

More recently, studies have shown promising prospects for a novel application of space tethers: electrodynamic propulsion.[8] To face the increasingly alarming issue of artificial space debris, it has been proposed to run ionospheric electrons down a conductive tether so that the resulting Lorentz force would decay the orbit of spent rocket stages and dysfunctional satellites much faster than air drag.

To study the long-term evolution of orbital elements and attitude dynamics of conductive space tethered systems, in this paper the authors extend their model presented in Ref. 7 to account for the influence of the Lorentz force on the satellite. The Earth's magnetic field is modeled by using a Legendre expansion in spherical coordinates (see Ref. 9) similar to that used to represent the Earth's gravitational field.

The performance of the two types of tethers (insulated and bare) is studied. The behavior of insulated systems is modeled based on the Parker–Murphy law,[10] modified following the flight of the TSS-1R in February 1996 (Ref. 11), whereas that of bare tethers is modeled after the treatment of Sanmartin et al.[12] The results were obtained by numerically integrating the equations governing the evolution of equinoctial elements that have no restrictions regarding eccentricity or inclination.

In the following a dynamic model of a tethered system is presented that includes the calculation of electrodynamic forces. Numerical results for an example are then given, followed by some concluding remarks.

Dynamic Model

Description of the System and of the Model

The system under consideration consists of two satellites linked by an axially extensible tether. The state of the tethered system is characterized by a set of 10 variables that describe the position and velocity of the center of mass of the system, the orientation and axial elongation of the tether, and its temperature. The position

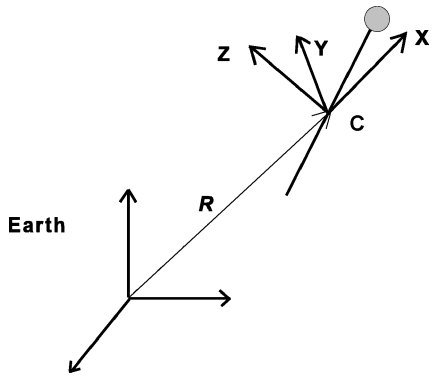

Fig. 1 Orbital coordinate axes.

and velocity of the system are obtained from a set of orbital elements defined later. The attitude of the tether is given by the in-plane pitch angle α and the out-of-plane roll angle γ. The longitudinal elongation of the tether is characterized by its strain (assumed uniform along the tether).

Most of the vectors needed for this analysis are easily expressed in orbital coordinates $OXYZ$. The origin of this noninertial coordinate system is the center of mass of the tethered satellite system (Fig. 1). The X axis is parallel to the local vertical, that is, along the position vector of the system center of mass measured from the center of the Earth. The Z axis points in the direction of the angular momentum vector of the satellite orbit. Finally, the Y axis completes the right-handed frame $OXYZ$.

In Refs. 6 and 7, a detailed formulation is presented to predict the trajectory and the attitude of the system, as well as the temperature and the longitudinal vibrations of the tether. That formulation will be adapted to the present case. It uses equinoctial elements $(a, P_1, P_2, Q_1, Q_2, L)$ for orbit propagation,[13] which are robust for small inclination and eccentricity. The mean longitude is replaced by true longitude of L^* for computational advantage. The equinoctial elements are related to the classical orbital elements as follows[13]:

$$P_1 = e\sin(\omega+\Omega), \qquad P_2 = e\cos(\omega+\Omega) \tag{1a}$$

$$Q_1 = \tan(i/2)\sin\Omega, \qquad Q_2 = \tan(i/2)\cos\Omega \tag{1b}$$

$$L^* = \theta + \omega + \Omega \tag{1c}$$

where a, e, i, ω, Ω, and θ are the classical orbital elements: These are semimajor axis, eccentricity, orbit inclination, argument of the perigee, longitude of the ascending node, and true anomaly, respectively.

The perturbation equations for the equinoctial elements can be written as

$$\dot{a} = (2a^2/h)\left[\left(P_2\sin L^* - P_1\cos L^*\right)f_x + (p/R)f_y\right] \tag{2a}$$

$$\dot{P}_1 = (R/h)\left\{-(p/R)\cos L^* f_x + \left[P_1 + (1+p/R)\sin L^*\right]f_y - P_2\left(Q_1\cos L^* - Q_2\sin L^*\right)f_z\right\} \tag{2b}$$

$$\dot{P}_2 = (R/h)\left\{(p/R)\sin L^* f_x + \left[P_2 + (1+p/R)\cos L^*\right]f_y + P_1\left(Q_1\cos L^* - Q_2\sin L^*\right)f_z\right\} \tag{2c}$$

$$\dot{Q}_1 = (R/2h)\left[1+Q_1^2+Q_2^2\right]\sin L^* f_z \tag{2d}$$

$$\dot{Q}_2 = (R/2h)\left[1+Q_1^2+Q_2^2\right]\cos L^* f_z \tag{2e}$$

$$\dot{L}^* = (h/R^2) - (R/h)\left(Q_1\cos L^* - Q_2\sin L^*\right)f_z \tag{2f}$$

where R, p, and h are the geocentric altitude of the center of mass of the tethered system, semilatus rectum, and specific angular momentum, respectively, whereas f_x, f_y, and f_z are the components of the perturbative acceleration along the orbital coordinate axes. Derivative with respect to time is represented by the dot.

The equations governing the pitch, roll, and longitudinal extension are

$$(\ddot{\alpha}+\ddot{\theta}) + 2(\dot{\alpha}+\dot{\theta})[(\bar{m}\dot{\ell}_0/m_e\ell_0) - \dot{\gamma}\tan\gamma + \dot{\epsilon}/(1+\epsilon)] + (3\mu/R^3)\sin\alpha\cos\alpha = Q_\alpha \tag{3a}$$

$$\ddot{\gamma} + 2\dot{\gamma}[(\bar{m}\dot{\ell}_0/m_e\ell_0) + \dot{\epsilon}/(1+\epsilon)] + \lfloor(\dot{\theta}+\dot{\alpha})^2 + (3\mu/R^3)\cos^2\alpha\rfloor\sin\gamma\cos\gamma = Q_\gamma \tag{3b}$$

$$[\ddot{\ell}_0(1+\epsilon) + 2\dot{\ell}_0\dot{\epsilon} + \ell_0\ddot{\epsilon}] + EA(\epsilon+\beta\dot{\epsilon}) - \left(m_e\big/m^*\right)\ell_0(1+\epsilon) \times [(\dot{\alpha}+\dot{\theta})^2\cos^2\gamma + \dot{\gamma}^2 + (\mu/R^3)(3\cos^2\alpha\cos^2\gamma - 1)] = Q_\epsilon \tag{3c}$$

where α, γ, and ϵ are the pitch angle, roll angle and longitudinal strain, respectively, ℓ_0 is the nominal length, and Q_α, Q_γ, and Q_ϵ are nondimensional generalized forces. Here m_e, $\bar{m}$, and m^* are functions of tether and end masses.[7]

The perturbative accelerations in Eqs. (2a–2f) and the generalized forces in Eqs. (3a–3c) arise due to the atmospheric lift and drag, asphericity of the Earth (zonal and sectorial harmonics), solar and albedo radiation, lunisolar attraction, and electrodynamic forces. Only the last one is discussed here. The details of the other forces may be found in Ref. 7; the only things that need to be mentioned here are that the World Geodetic System 1984 (WGS84) model is used for the gravitational field and Jacchia J-77 model[14] for atmospheric density. The orbit propagation results presented in this paper, of course, include all effects.

To determine the generalized forces, the tethered system is discretized into $k+2$ elements: two for the end bodies and k elements for the tether. The principle of virtual work is used to obtain the generalized forces in Eqs. (3a–3c). The quantities f_x, f_y, and f_z are determined by adding all of the environmental forces acting on the $k+2$ elements and dividing by the total mass of the system.

Electromagnetic Field

The magnetic field of the Earth at any point can be described in terms of a series of associated Legendre polynomials in spherical coordinates as follows[9]:

$$B_R = \sum_{k=1}^{\infty}\frac{R_\oplus^{k+2}}{R^{k+2}}\sum_{j=0}^{k}(k+1)P_k^j[s(\phi)]\left[g_k^j\Psi_1 + h_k^j\Psi_2\right] \tag{4a}$$

$$B_\lambda = \sec(\phi)\sum_{k=1}^{\infty}\frac{R_\oplus^{k+2}}{R^{k+2}}\sum_{j=0}^{k}jP_k^j[s(\phi)]\left[-g_k^j\Psi_2 + h_k^j\Psi_1\right] \tag{4b}$$

$$B_\phi = \sum_{k=1}^{\infty}\frac{R_\oplus^{k+2}}{R^{k+2}}\sum_{j=0}^{k}P_k'^j[s(\phi)]\left[g_k^j\Psi_1 + h_k^j\Psi_2\right] \tag{4c}$$

where the prime above P denotes differentiation with respect to its argument. The values of g and h are found in the International Geomagnetic Reference Field (IGRF) model.[15]

The electromotive force induced in a conductive space tethered system is given by[2]

$$Y = \int_{\text{system}}(\boldsymbol{v}_{s/m}\times\boldsymbol{B})\cdot\,\mathrm{d}\boldsymbol{l} \tag{5}$$

where the velocity of the satellite element with respect to the magnetic fields, $\boldsymbol{v}_{s/m}$, is given by

$$\boldsymbol{v}_{s/m} = \boldsymbol{v}_s - \omega_\oplus\times\boldsymbol{R} \tag{6}$$

where $\boldsymbol{v}_s$ is the absolute velocity of the element and $\omega_\oplus$ is the angular velocity of the Earth's magnetic field.

Current in an Insulated Tether

Conducting tethers can be either insulated (with inner conducting core covered by an insulator) or bare (with conducting section

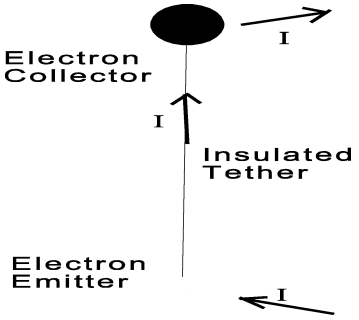

Fig. 2 Current flow in an insulated conductive tether.

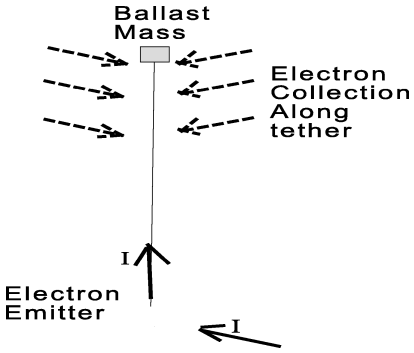

Fig. 3 Current flow in a bare conductive tether.

exposed directly to the ionosphere). In this subsection, the characteristics of insulated wire systems are analyzed. These devices can only exchange electrons with the ionosphere using the subsatellites because the entire wire is covered with an insulator (Fig. 2). As a result, electron collection in insulated systems is limited to fairly low currents due to Debye-sheath shielding (see Refs. 12 and 16). On the other hand, electron emission can be achieved using a hollow cathode or an electron gun.

As in other investigations,[12,16–18] the present formulation neglects the tether resistance and assumes perfect efficiency. The short-circuit current, which corresponds to a load resistance of 0, is given by the Parker–Murphy law,[10] which was recently updated following the TSS-1R mission[11]:

$$I_{\max} \approx K_1 n_e T_\infty^{\frac{1}{2}} \left[\tfrac{1}{2} + (Y/Y_0)^{0.528}\right] \tag{7}$$

where $K_1 = 5.1255 \times 10^{-15}$ A $\cdot$ m^3/(K)$^{1/2}$ and n_e is the ionospheric electron density which varies between 10^{12} e$^-$/m^3 (during the day) and 10^{10} e$^-$/m^3 (at night). T_∞ is the undisturbed ionospheric plasma temperature, Y is the electromotive force given by Eq. (5), and Y_0 is given by

$$Y_0 = A^* B^2 \mathrm{e}^- \big/ 8\pi m_e \tag{8}$$

Here A^* is the total surface area of the collecting body, B is the magnitude of the surrounding magnetic field, e$^-$ is the elementary electron charge, and m_e is the electron mass.

Tether Current in a Bare Tether

Bare wire systems rely on the tether itself for electron collection (Fig. 3). However, a bare wire cannot effectively release electrons into the ionosphere.[18] For this reason, such systems must be equipped with one subsatellite acting as an electron emitter and another end mass that merely serves as a ballast to keep the tether taut. Unlike insulated tethers, the characteristic radius of bare wire systems, that is, the tether radius, is much smaller than the Debye gyroradius. This virtually eliminates Debye shielding, which severely limits the electron collection capability of insulated systems. As a result, bare tethers can collect ions in much larger numbers than

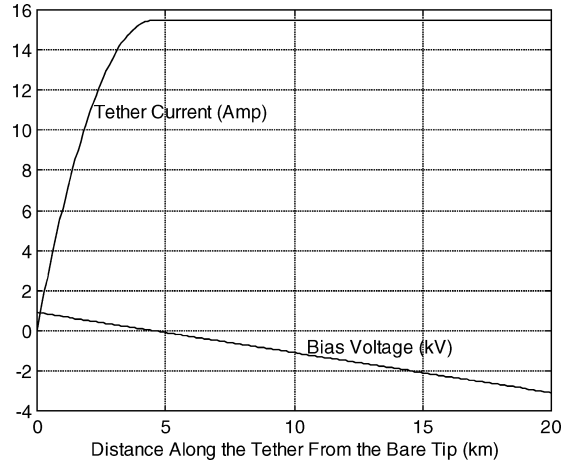

Fig. 4 Current and bias voltage variation along a bare conductive tether.

insulated wire systems.[16] Bare tethers are also less affected by large variations in electron density than insulated systems.

For example, Fig. 4 shows the voltage bias and the tether current along a bare wire system designed for the generation of 3.1 kW through a load resistance of 200 Ω using a 20-km-long tether with a 1 mm radius flying through a motional electric field $E_0 = 0.2$ V/m and an electron density of 9×10^{11} e$^-$/m^3. The voltage bias V^* is defined as the difference between the motional emf generated at a distance l from m_1 and the voltage drop/rise at the load/battery.[16] In other words,

$$V^*(l) = E_0 l - I_{\max} R_{\text{load}} \tag{9}$$

In Eq. (9), the motional electric field E_0 is the ratio of the total emf across the system over the total tether length.

The collection scenario is the following: The electrons are captured over a segment of the tether (4.52 km in Fig. 4). Beyond this point, the current reaches its maximum value (15.48 A in Fig. 4) and does not change thereafter because the voltage bias becomes negative and the wire does not effectively release electrons.

In mathematical terms, electron collection in bare wires takes place according to the following relations.[12,16] For the interval along the tether where the voltage bias is positive, that is, from $l_{\text{tot}} - l_c$ to $l = l_{\text{tot}}$, we have

$$\frac{\mathrm{d}I(l)}{\mathrm{d}l} = K_2 n_e r_t [V^*(l)]^{\frac{1}{2}} \tag{10}$$

where $V^*(l)$ is given by Eq. (9) and $K_2 = 1.9 \times 10^{-13}$ (C^3/kg)$^{1/2}$. On integration, the differential equation (10) yields

$$I(l) = \tfrac{2}{3} K_2 r_t n_e (E_0)^{\frac{1}{2}} \left\{ l_c^{\frac{3}{2}} - [l - (I_{\max} R_{\text{load}})/E_0]^{\frac{3}{2}} \right\} \tag{11}$$

In Eq. (11), the electron collection length l_c is given by

$$l_c = l_{\text{tot}} - I_{\max} R_{\text{load}} / E_0 \tag{12}$$

For the interval along the tether for which the voltage bias is negative, that is, from $l = 0$ to $l = l_{\text{tot}} - l_c$, the tether current is constant,

$$I(l) = I_{\max} = \tfrac{2}{3} K_2 r_t n_e (E_0)^{\frac{1}{2}} l_c^{\frac{3}{2}} \tag{13}$$

To verify the validity of Eq. (11), one can note that it yields zero current when $l = l_{\text{tot}}$ and maximum current when $l = l_{\text{tot}} - l_c$, which agrees with Fig. 4.

Electrodynamic Force

The current flow through the tether (whether it is insulated or bare) induces a Lorentz force on the system (Ref. 2), which is given by

$$F_{\text{mag}} = \int_0^{l_{\text{tot}}} I(\mathrm{d}\boldsymbol{l} \times \boldsymbol{B}) \tag{14}$$

For insulated wire tethers, the current I can be taken out of the preceding integral because it remains uniform across the system. The magnetic field vector is given by Eq. (4). For insulated systems, the tether current is given by Eq. (7), whereas for bare systems, the current is given by Eqs. (11) or (13), depending on the position along the tether.

Lorentz forces are responsible for the progressive decay of the tethered satellite orbit when the system works as an electrical generator. On the other hand, using a battery to run current against the induced emf produces a thrust, which raises the orbit of the system. However, this thrust is produced at the expense of the energy provided by the battery. By proper modulation of the current in the tether, the electrodynamic force can also be used to control the rotational motion of the tether. Such modulation can be achieved with a variable load resistance and with a battery that reverses the direction of the current when necessary.

Analysis and Results

Satellite Parameters for Simulation

Simulations of the dynamic behavior of a satellite carrying an electrodynamic tether and a small auxiliary end mass were carried out by integrating Eqs. (2) and (3) numerically using Gear's method[19] suitable for "stiff" systems. The system is numerically stiff because the orbital elements change much slowly compared to α, γ, and ϵ. The simulations assume that the center of mass of the tethered system of interest initially orbits the Earth along a circular orbit. The end bodies measure ($0.5 \times 0.8 \times 0.6$ m^3) and ($0.05 \times 0.08 \times 0.06$ m^3), respectively, and have a mass of 50 and 5 kg, respectively. The length of the tether is 20 km. The load resistance is neglected. The tether core has a radius of 0.2 mm, and it is made of aluminum (2219-T851), which has a density of 2850 kg/m^3 and a resistivity of $27.4 \times 10^{-9}\ \Omega \cdot$ m. The ionospheric plasma temperature is assumed to be 1000 K, whereas the electron density profile is $(0.9 \sin\theta + 1.1) \times 10^{12}$ e$^-$/m^3.

EMF, Current, and Lorentz Forces in Insulated and Bare Tether Systems

Figures 5–8 show the variation in the induced emf, collected current, and Lorentz forces for bare and insulated systems. In these simulations, the satellite of interest (bigger end mass) is assumed to fly 600 km above the surface of the Earth, with the tether aligned along the local vertical. As seen in Figs. 5 and 6, the induced emf increases linearly with the tether length and is unaffected by the insulated or bare nature of the tether. On the other hand, the induced current at m_1 and the Lorentz forces are one to two orders of magnitude larger for bare tethers than for insulated tethers. As mentioned in the "Dynamic Model" section, this is the consequence of the Debye shielding in insulated systems, and the results clearly demonstrate the superior capability of bare tethers to capture ionospheric electrons.

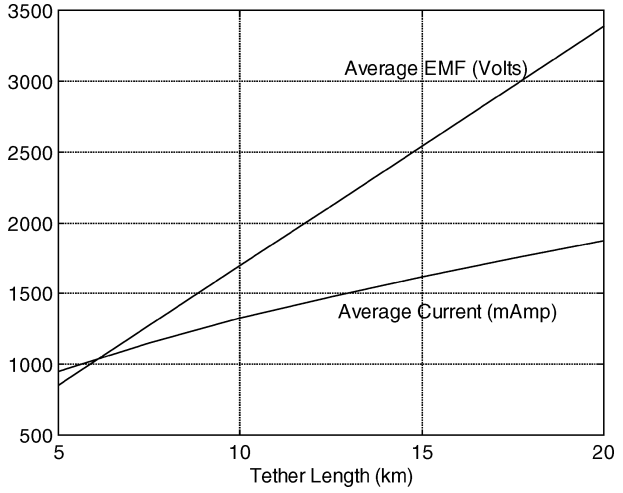

Fig. 5 Typical average emf and current in an insulated tethered system.

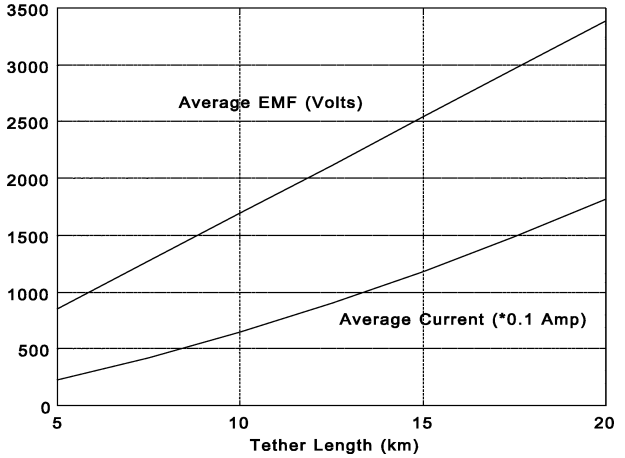

Fig. 6 Typical average emf and current at the main mass m_1 in a bare tethered system.

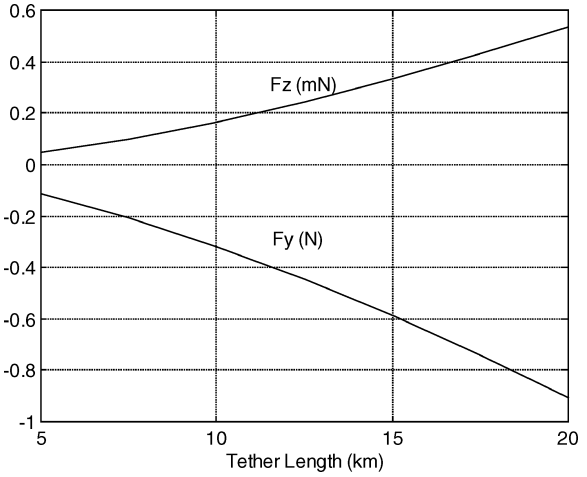

Fig. 7 Average Lorentz forces induced in an insulated tethered system.

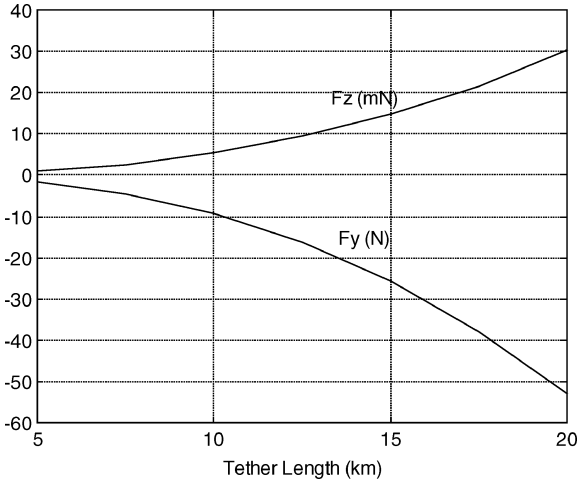

Fig. 8 Average Lorentz forces induced in a bare tethered system.

Effect of Orbital Inclination on Lorentz Forces

The effect of the orbital inclination on Lorentz forces and related quantities is shown in Figs. 9–12. The orbital inclination strongly influences the average voltage, current, and Lorentz forces. As a matter of fact, the emf and current reverse direction in retrograde orbits. Furthermore, the magnitude of the induced emf or induced current reaches a minimum along nearly polar orbits and is larger

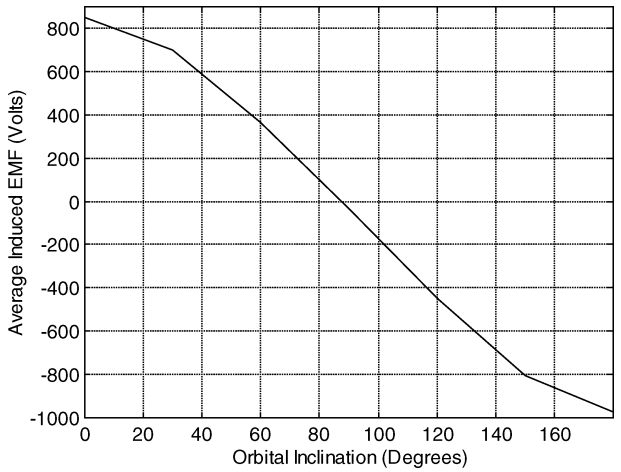

Fig. 9 Variation of the average induced emf with orbital inclination.

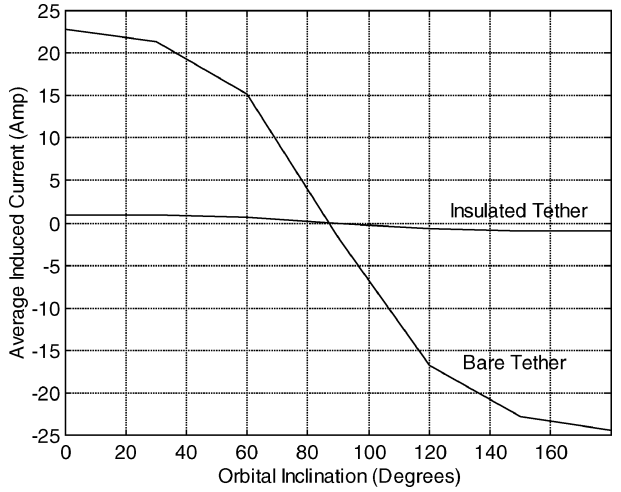

Fig. 10 Variation of the average current at m_1 with orbital inclination.

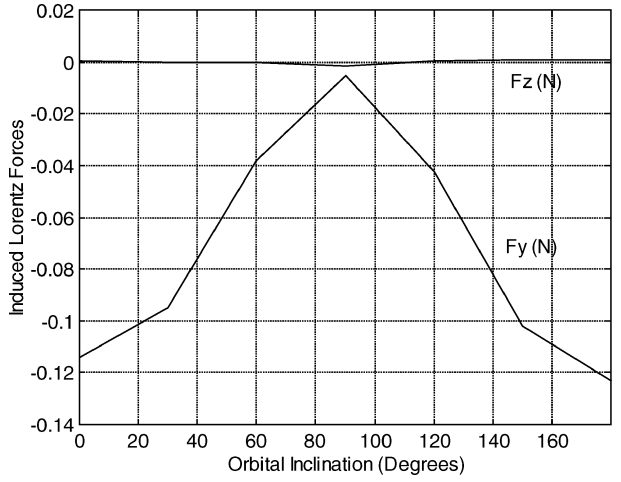

Fig. 11 Variation of induced Lorentz forces with orbital inclination for an insulated tethered system.

for inclination of $\pi - i$ than i. Indeed, the speed of the satellite with respect to a frame moving with the magnetic field of the Earth is larger for retrograde orbits than for direct orbits. As per Eqs. (5), (7), (13), and (14) this generates larger emfs, currents, and Lorentz forces.

In light of the results presented so far in this section, the average value of F_y has been shown to always remain negative. The explanation for this is quite simple: The electrodynamic force has the tendency of bringing any conductive object to "rest" with respect to a coordinate system with its origin at the center of the Earth and rotating with the magnetic field. Whether its trajectory is direct or retrograde, any satellite system moving at orbital speeds in low Earth orbit (LEO) is bound to travel much faster than the magnetic field (400–500 m/s at the equator).

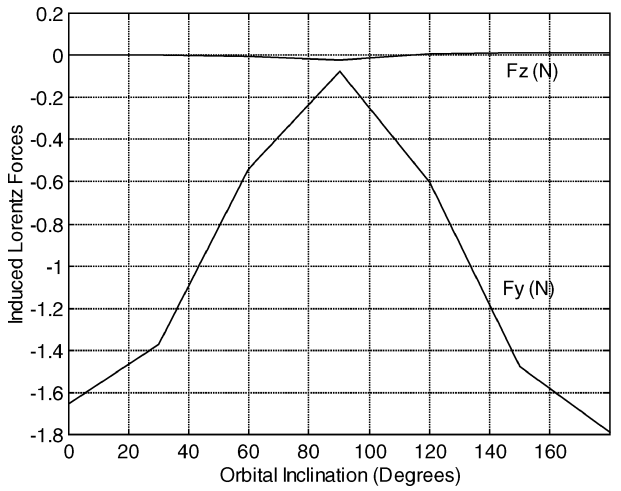

Fig. 12 Variation of induced Lorentz forces with orbital inclination for a bare tethered system.

Orbit Boost Using Electrodynamic Tethers

The preceding results imply that regardless of the inclination, it is impossible to raise the orbit of a satellite in a low Earth circular orbit by continually applying maximum electrodynamic thrust. In fact, a circular orbit can be raised only if the average tangential y component of the perturbative force is positive. For altitudes beyond the geostationary orbit, the speed of the magnetic field becomes greater than the orbital speed. A satellite traveling along one such trajectory could potentially use the magnetic field of the Earth to obtain both thrust and "free" electrical power. However, the low intensity of the magnetic field at these altitudes may very well undermine the potential of this application. On the other hand, this concept could turn out to be very attractive for propelling a spacecraft in orbit around Jupiter: a planet with a very strong magnetic field and most of its moons above the "jupitostationary" orbit.

This leaves only one possible way of using electrodynamic forces to raise the orbit of a LEO satellite: emf reversal. This procedure consists of using a series of batteries to reverse the direction of the induced emf and provide a positive F_y. The PMG experiment[2] constitutes the only example of such emf reversal. Indeed, the planners of this mission connected several batteries in series to generate an emf of approximately 80 V, which was higher than the voltage induced by the motion of the 500-m tether through the magnetic field. However, one could use a dual tether, with one conductive section and another nonconductive part. This would keep the tether taut and ensure that the battery does not have to work against unreasonably large motional emfs.

Orbit Decay Using Electrodynamic Tethers

As mentioned in the Introduction, the tethered deorbit concept proposes to capitalize on the electrodynamic thrust generation to decay the orbit of dysfunctional satellites and spent rocket stages. The range of tether lengths required to keep the tether taut (>5 km) allows the flow of very high currents (0.5–5 A) through the tether with emfs in the kilovolt range. If uncontrolled, these high currents generate large Lorentz torques that destabilize the librations of the system.[6] Stabilizing tether librations while decaying the satellite orbit as rapidly as possible requires a sophisticated control system. Although far from optimal, the control scheme chosen for the following simulations is relatively simple. It consists of an ammeter and a varistor working in concert to keep the maximum current at $I = [(0.2 + 0.1\sin(3\theta)]$ A. The 3θ dependency helps contain roll oscillations. To further suppress libration amplitudes, the tether current is cut whenever pitch or roll reaches an amplitude larger than 20 deg.

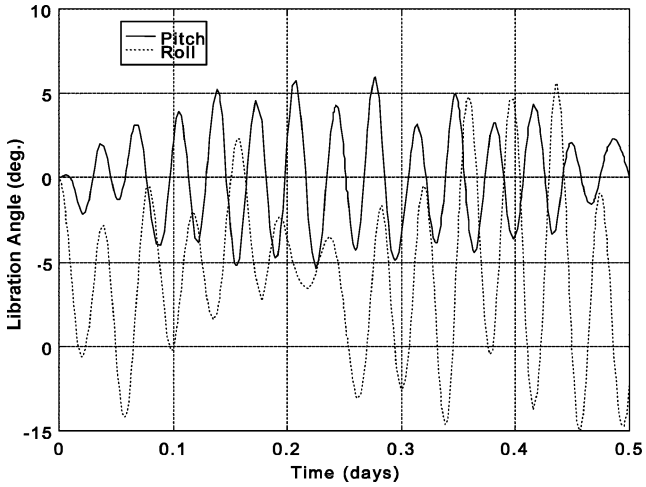

Fig. 13 Librations of conductive tethered system in a circular orbit at 1500-km altitude; $i = 0$ deg.

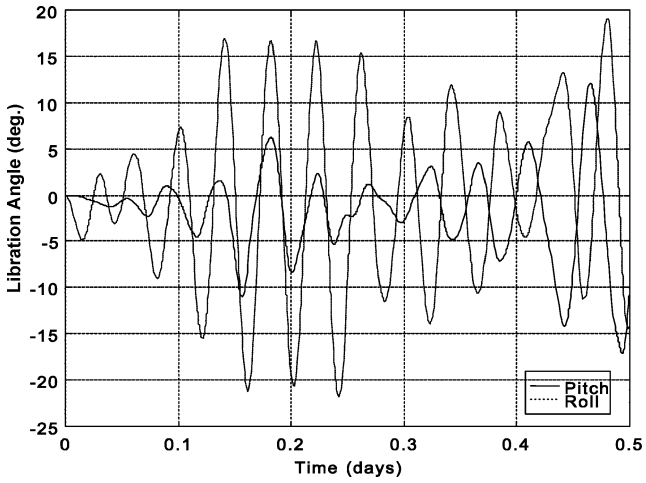

Fig. 14 Librations of a conductive tethered system in a circular orbit at 1500-km altitude; $i = 85$ deg.

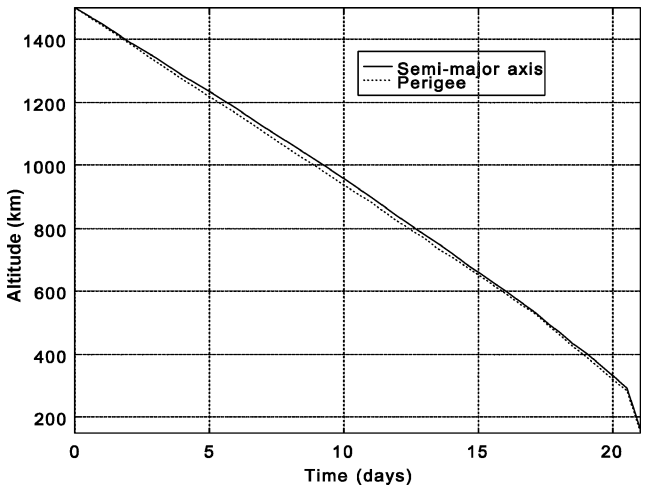

Fig. 15 Orbital decay of a satellite initially in a circular orbit at 1500-km altitude; $i = 0$ deg.

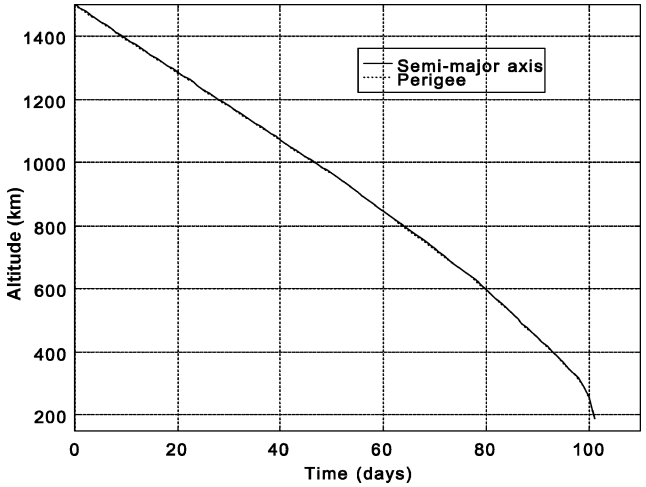

Fig. 16 Orbital decay of a satellite initially in a circular orbit at 1500-km altitude; $i = 85$ deg.

Because the superior potential of bare tethers has already been established, the simulations presented in this subsection assume that the satellite is equipped with a 5-km-long bare tether.

To demonstrate the effectiveness of the proposed current/libration control scheme, Figs. 13 and 14 show the controlled librations of a deorbit tether flying at an altitude of 1500 km along a circular orbit for two different inclinations: 0 deg (Fig. 13) and 85 deg (Fig. 14). Note that the libration amplitudes barely exceed 20 deg in both pitch and roll. Hence, the described control scheme effectively stabilizes tether librations.

Let us now examine how rapidly electrodynamic propulsion (EP) can decay the orbit of a given object. Although several orbital elements change, the evolution of the semimajor axis and perigee is relevant here. Figure 15 presents that evolution for the example satellite, whose parameters and current control system are presented earlier. The satellite initially orbits along an equatorial and circular orbit at an altitude of 1500 km. For this system, the deorbit time is 21 days.

As pointed out by Hoyt and Forward,[20] deorbit rates decrease drastically for nearly polar orbits because the magnetic field orientation is unfavorable to orbit decay near polar latitudes. This phenomenon is exemplified in Fig. 16, which shows how the semimajor axis and perigee take much longer to decay for a similar satellite initially flying along a circular orbit at an altitude of 1500 km and inclination of 85 deg.

In Figs. 15 and 16, one notices that the semimajor axis and perigee decay smoothly over most of the maneuver (when Lorentz forces dominate), but drop at an increasing rate near the end of the flight (when air drag becomes dominant). Deorbit times of 21 days (for an equatorial orbit) and 101 days (for a nearly polar orbit) compare extremely well with the dozens to hundreds of years required for air drag alone to decay the satellite orbit. On the other hand, the reentry time for rocket propulsion is half of the orbital period (approximately 1 h), much less than both EP and air drag.

The ballast and conductive tether total 20 kg of the total system mass. This result is independent of the control scheme used to reduce tether librations. Indeed, the current control system only influences the deorbit time, not the tether system mass. This 20 kg exceeds the 5.6 kg of hydrazine–N_2O_4 fuel required to deorbit the 50-kg satellite chemical propulsion. Therefore, EP is not as good as rocket propulsion to deorbit very small satellites in LEO. However, the same EP system (a 5-kg tether measuring 5 km with a 5-kg ballast) can deorbit a 1000-kg satellite initially flying along a 1500-km circular and equatorial orbit within 380 days. In fact, for a given control system, the deorbit time is inversely proportional to the satellite mass. On the other hand, a rocket system designed to accomplish a comparable task would require more than 110 kg of fuel. Further analysis reveals that for the current control scheme and rocket fuel described, Lorentz forces are more weight efficient than chemical rocket propulsion when the satellite mass is larger than 90 kg.

Conclusions

A model to analyze the long-term dynamics of orbital tethered systems was presented. Particular emphasis was placed on the effect

of electrodynamic (Lorentz) forces on the system. The motional emf, the induced current, and the resulting Lorentz forces were derived for both insulated and bare tethered systems.

The bare wires are much more efficient at collecting ionospheric ions than insulated tethers. Hence, bare tethers can provide larger electrodynamic force for a given mass of tether. Furthermore, other parameters such as tether length and resistivity, altitude, and inclination greatly influence the Lorentz forces on a satellite.

Raising the orbit of a satellite is possible if a reasonably short part of the tether is conductive (to ensure that the satellite battery does not have to fight against unreasonably large emfs) and if the other part is nonconductive (to ensure that the tether remains taut).

Furthermore, Lorentz forces can be effectively used to decay the orbit of a satellite. For the particular control system described in this paper, Lorentz forces are more effective for orbital decay than chemical rocket propulsion when the satellite mass is larger than approximately 100 kg. However, the reentry time for deorbit tethers (weeks to months) largely depends on the libration control scheme and is much longer than that of rocket systems (1 h) but still much faster than air drag alone (dozens to hundreds of years).

Acknowledgments

The work presented in this paper was supported by the Natural Sciences and Engineering Research Council of Canada (NSERC), the Canadian Space Agency through an NSERC supplement, Bristol Aerospace, and the Fonds pour la formation de chercheurs et l'aide à la recherche.

References

[1]Hacker, B. C., and Alexander, C. C., *On the Shoulders of Titans: A History of Project Gemini*, NASA Special Publication 4203, NASA History Series, 1977, pp. 361, 366–368, 378, 379.

[2]Cosmo, M. L., and Lorenzini, E. C., *Tethers in Space Handbook*, 3rd ed., NASA Marshall Space Flight Center and Smithsonian Astrophysical Observatory, 1997.

[3]Raitt, W. J., *Sounding Rocket Tethered Experiments: The NASA CHARGE Program*, Proceedings of the Fourth International Conf. on Tethers in Space, Vol. 1, Smithsonian Inst., Washington, DC, 1995, pp. 107–118.

[4]Misra, A. K., and Modi, V. J., "A Survey on the Dynamics and Control of Tethered Satellite Systems," *Advances in the Astronautical Sciences*, Vol. 62, 1987, pp. 667–719.

[5]Purdy, W., Coffey, S., Barnds, W. J., Kelm, B., and Davis, M., "TiPS: Results of a Tethered Satellite Experiment," American Astronautical Society, Paper AAS-97-600, Aug. 1997.

[6]Lanoix, E. L. M., "A Mathematical Model for Long Term Dynamics of Tethered Satellites Systems," M.S. Thesis, Dept. of Mechanical Engineering, McGill Univ., Montreal, June 1999.

[7]Lanoix, E. L. M., Misra, A. K., Modi, V. J., and Jablonski, A. M., "A Mathematical Model for Long-Term Orbit and Attitude Propagation of Tethered Satellites Systems," 49th International Astronautical Congress, Paper IAF-98-A.7.04, Sept.–Oct. 1998.

[8]Forward, R. L., Hoyt, R. P., and Upoff, C., "Application of the Terminator Tether Electrodynamic Drag Technology to Deorbit of Constellation Spacecraft," AIAA Paper 98-3491, 1998.

[9]Langel, R. A., "Main Field," *Geomagnetism*, edited by J. A. Jacobs, Academic Press, London, 1987, pp. 249–512.

[10]Parker, L. W., and Murphy, B. L., "Potential Buildup on an Electron-Emitting Satellite," *Journal of Geophysical Research*, Vol. 72, No. 5, 1967, pp. 1631–1636.

[11]Thompson, D. C., Bonifazi, C., Gilchrist, B. E., Williams, S. D., Raitt, W. J., Lebreton, J.-P., and Burke, W. J., "The Current-Voltage Characteristics of a Large Probe in Low Earth Orbit: TSS-IR Results," *Geophysical Research Letters*, Vol. 25, No. 4, 1998, pp. 415–418.

[12]Sanmartin, J. R., Martinez-Sanchez, M., and Ahedo, E., "Bare Wire Anodes for Electrodynamic Tethers," *Journal of Propulsion and Power*, Vol. 9, No. 3, 1993, pp. 353–360.

[13]Battin, R. H., *An Introduction to the Mathematics and Methods of Astrodynamics*, AIAA Education Series, AIAA, Washington, DC, 1987, pp. 490–493.

[14]Jacchia, L. G., "Thermospheric Temperature, Density, and Composition: New Models," Smithsonian Astrophysical Observatory, Special Rept. 375, Cambridge, MA, March 1977.

[15]International Association of Geomagnetism and Aeronomy Division V, Working Group 8, "International Geomagnetic Reference Field, 1995 Revision," *Journal of Geomagnetism and Geoelectricity*, Vol. 47, 1995, pp. 1257–1261.

[16]Estes, R. D., Sanmartin, J. R., and Martinez-Sanchez, M., "Technology of Bare Tether Current Collection," Tether Technology Interchange Meeting, NASA Marshall Space Flight Center, Hunstville, AL, Sept. 1997.

[17]Johnson, L., and Herrmann, M., "International Space Station Electrodynamic Tether Reboost Study," NASA TM-1998-208538, July 1998.

[18]Lorenzini, E. C., Estes, R. D., and Cosmo, M. L., "Electrodynamic Tethers for the International Space Station," *In-Space Transportation with Tethers*, Annual Rept. for NASA Grant NAG9-1303, Smithsonian Astrophysical Observatory, Cambridge, MA, Oct. 1997, pp. 4–23.

[19]Gear, C. W., *Numerical Initial Value Problems in Ordinary Differential Equations*, Prentice–Hall, Englewood Cliffs, NJ, 1971.

[20]Hoyt, R., and Forward, R., "Performance of the Terminator Tether™ for Autonomous Deorbit of LEO Spacecraft," AIAA Paper 99-2839, June 1999.